Bioscience Reports (2020) **40** BSR20201854
https://doi.org/10.1042/BSR20201854

Research Article

Ultrasonic irradiation and SonoVue microbubbles-mediated RNA interference targeting PRR11 inhibits breast cancer cells proliferation and metastasis, but promotes apoptosis

Hui Luo[1,2,*], Jian Li[1,2,*], Qi Lin[1,2], Xiaojun Xiao[1,2], Yang Shi[1,2], Xiuqin Ye[1,2], Zhanghong Wei[1,2], Yingying Liu[1,2] and Jinfeng Xu[1,2]

[1]Department of Ultrasound, Shenzhen People's Hospital, The Second Clinical Medical College of Jinan University, Shenzhen, China; [2]Shenzhen Medical Ultrasound Engineering Center, Shenzhen People's Hospital, The Second Clinical Medical College of Jinan University, Shenzhen, China

Correspondence: Jinfeng Xu (xujinf_jinfeng@163.com)

The present study compared the effects of ultrasonic irradiation and SonoVue microbubbles (US) or Lipofectamine 3000 on the transfection of small interfering RNA for PRR11 (siPRR11) and Proline-rich protein 11 (PRR11) overexpression plasmid into breast cancer cells. SiPRR11 and PRR11 overexpression plasmid were transfected into breast cancer MCF7 cells mediated by US and Lipofectamine 3000. PRR11 expressions in breast cancer and normal tissues were determined using Gene Expression Profiling Interactive Analysis (GEPIA). The viability, proliferation, migration, invasion and apoptosis of breast cancer cells were respectively measured by MTT assay, clone formation assay, scratch wound-healing assay, Transwell assay and flow cytometry. PRR11 and epithelial-to-mesenchymal transition (EMT)-related and apoptosis-related (B-cell lymphoma 2, Bcl-2; Bcl-2-associated protein X, Bax) proteins' expressions were detected by quantitative real-time polymerase chain reaction (qRT-PCR) and Western blot as appropriate. As ultrasonic intensity increased, the viability of MCF7 cells was decreased. Results from GEPIA suggested that PRR11 was up-regulated in breast cancer. Silencing PRR11 mediated by US showed a higher efficiency than by Lipofectamine 3000. SiPRR11 transfected by Lipofectamine 3000 suppressed cells growth and metastasis, while promoted cell apoptosis. Moreover, E-cadherin (E-cad) and Bax expressions were high but N-cadherin (N-cad), Snail and Bcl-2 expressions were low. However, overexpressed PRR11 caused the opposite effects. More importantly, transfection of siPRR11 and PRR11 overexpression plasmid using US had a higher efficacy than using Lipofectamine 3000. US transfection of PRR11 siRNA showed better effects on inhibiting breast cancer progression. The current findings contribute to a novel treatment for breast cancer.

[*]These authors contributed equally to this work.

Received: 27 May 2020
Revised: 29 September 2020
Accepted: 09 October 2020

Accepted Manuscript online: 15 October 2020
Version of Record published: 02 November 2020

Introduction

At present, breast cancer remains one of the most frequent malignancies and also a common cause of cancer-related mortality among females around the world. According to clinical outcomes and biological behaviors, breast cancer is a highly heterogeneous disease that can be further classified into different subtypes according to various criteria [1]. Though the screening, diagnosis and treatment of breast cancer have progressed greatly, approximately 12% of patients develop metabolic diseases, resulting in poor prognosis [2]. Thus, potential therapeutic methods are still urgently needed for a better treatment of breast cancer.

Bioscience Reports (2020) **40** BSR20201854
https://doi.org/10.1042/BSR20201854

Proline-rich protein 11 (PRR11), located on 17q22 region of human chromosome, is implicated in the transduction of cell signal and events to cancer-onset [3]. Increasing evidence suggested that PRR11 is involved in the development and progression of many malignancies. Huang et al. found that PRR11 contributes to the pathogenesis of non-small cell lung cancer (NSCLC), and knockdown on PRR11 suppresses the proliferation and metastasis of NSCLC cells and promotes the cell apoptosis [4]. Moreover, the up-regulation of PRR11 expression is an unfavorable prognostic factor in tongue squamous cell carcinoma (TSCC) [5]. In breast cancer, Wang et al. showed that PRR11 is overexpressed in breast cancer cells and have a negative prognostic value in breast cancer, knockdown of PRR11 inhibits breast cancer cell proliferation, migration, and invasion [6].

Currently, traditional gene transfection is generally achieved by viral or non-viral vectors [7]. However, further application on these factors is limited by the safety of viral vectors in human bodies and low transfection efficiency of non-viral vectors [8]. Recently, a study found that compared with microbubble injection of target genes, ultrasound radiation is remarkable in promoting transfection efficiency and in increasing gene expressions [9]. Agents for microbubble ultrasound contrast emerge as novel vectors for gene transfection, as they showed high safety, stability, and efficiency [10]. Microbubbles 'break' and release target gene under the energy from ultrasound radiation, which can increase cell permeability and create a reversible sound hole that promotes the infiltration of target genes into the nucleus and therefore increase gene transfection and expression efficiency [11,12]. In clinical practice, applying microbubble ultrasound agent in gene therapy has attracted much attention due to its high efficiency of transfection and low side effects [13].

Based on the possible oncogenic role of PRR11 in breast cancer development and progression [6], the present study explored the efficiency and safety of using ultrasonic irradiation and SonoVue microbubbles (US) in transfecting PRR11 into human breast cancer MCF7 cells. Moreover, the role of PRR11 in the development and progression of breast cancer and the feasibility of gene therapy using US were also investigated.

Materials and methods

Gene profiling analysis

To explore the role of PRR11 in breast cancer, PRR11 expression in breast cancer susceptibility gene (BRCA) were retrieved from Gene Expression Profiling Interactive Analysis (GEPIA) 2 (GEPIA2) (http://gepia.cancer-pku.cn/)

Cell culture and treatment

Human breast cancer cell line MCF7 (catalog no. HTB-22) was purchased from American Type Culture Collection (ATCC; Gaithersburg, MD, U.S.A.) and seeded in Roswell Park Memorial Institute (RPMI)-1640 medium (L1032; Biologos, Montgomery, IL, U.S.A.) supplemented with 10% fetal bovine serum (FBS; SFBU30, Equitech-Bio, Kerrville, TX, U.S.A.), 1% penicillin/streptomycin (09-757F, Lonza, Basel, Switzerland) at 37°C with 5% CO_2.

For transfection using microbubble and ultrasound, SonoVue was used as previously described [14]. Six fluorinated sulfur (SF_6) was purchased from Bracco (Milan, Italy) and used as the agent of SonoVue (average diameter: 2.5 μm). Five milliliters of saline solution and 50 μl small interfering RNA for PRR11 (siPRR11) and PRR11 overexpression plasmid were added into the SonoVue microbubble before the experiment.

For subsequent studies, MCF7 cells were divided into the following groups: Control group (normal culture without transfection), NC-L/siNC-L group (cells were transfected with negative control (NC) or small interfering RNA for NC (siNC) by using Lipofectamine 3000 reagent), NC-US/siNC-US group (cells were transfected with NC or siNC using US), siPRR11-L/PRR11-L group (cells were transfected with siPRR11 or PRR11 overexpression plasmid using Lipofectamine 3000 reagent), and siPRR11-US/PRR11-US group (cells were transfected with siPRR11 or PRR11 overexpression plasmid using US).

Transfection

SiPRR11 (A01004, sequence: 5′-ACUACAAAAUUAAAUCCUUGUC-3′) and its NC (A06001, sequence: 5′-ACAAUUGUCAAUUACUACUAAC-3′) were purchased from Gene Pharma (Shanghai, China) and transfected using Lipofectamine. PRR11 was successfully overexpressed using pEGFP-N1 plasmid (V12021; NovoPro, Shanghai, China). For cell transfection, 1×10^5 cells/well MCF7 cells were cultured in a 24-well plate to reach a confluence of 70–90%, and then transfected with 50 nmol siPRR11 and PRR11 overexpression plasmids, and NC using Lipofectamine 3000 reagent (L3000-015; Thermo Fisher Scientific, Waltham, MA, U.S.A.). Then, 48 h after transfection, transfection efficiency was detected by quantitative real-time polymerase chain reaction (qRT-PCR) and Western blot.

For the transfection using microbubble and ultrasound, the MCF7 cells (passages 3–5) were cultured in a 24-well plate at a density of 2×10^5 cells/ml (500 μl/well) at 37°C with 5% CO_2 overnight. A total of 450 μl non-serum and non-antibiotic RPMI-1640 medium were added into the cells after they reached 80% confluence, and then 50 μl SonoVue containing siPRR11 and PRR11 overexpression plasmid were added into each well. The concentration of SonoVue of the cells was adjusted to approximately 10%.

MTT assay

The MCF7 cells were divided into the following groups (0, 0.5, 0.75, 1, and 1.25 W/cm^2 groups) according to different ultrasonic intensities, and the cells were treated for 45 s. The MCF7 cells (1×10^5 cells/well) were then grown in 96-well plates and added with 10 μl MTT assay kit (#30006; Biotium, Beijing, China). A total of 100 μl dimethyl sulfoxide (DMSO; 85190, Thermo Fisher Scientific, U.S.A.) was added to dissolve formazan salt crystals after incubation at 37°C for 4 h. OD values at an absorbance of 490 nm were recorded using Multiskan FC Microplate Photometer (catalog no. 51119180ET, Thermo Fisher Scientific, U.S.A.).

Clone formation assay

The MCF7 cells (1×10^2 cells/well) were seeded in a six-well plate at 37°C with 5% CO_2) and then fixed by pure methanol for 15 min. After treatment for 2 weeks, the cells were stained by Crystal Violet for 30 min, and visible colonies were observed under a stereo microscope (SZX10; Olympus, Hangzhou, China). Images of each colony were photographed and clone formation was subsequently calculated.

Scratch assay

The MCF7 cells (1×10^5 cell/well) were seeded in 24-well plates after transfection for 48 h. After the cells reached approximately 80% confluence, the scratch was created using a sterile pipette tip, and the cells were further cultured in non-serum RPMI-1640 medium at 37°C with 5% CO_2. Cell images were captured under a stereo microscope (SZX10; Olympus, China) at 100× magnification at 0 and 24 h. Cell migration was detected and measured using Image-Pro Plus Analysis software 7.0 (Media Cybernetics, Rockville, MD, U.S.A.).

Transwell assay

The upper chamber of the Transwell (8-μm-pore, CLS3422, Sigma–Aldrich, U.S.A.) was pre-coated by 50 μl Matrigel (M8370; Solarbio, Beijing, China), and contained the transfected MCF7 cells at 37°C with 5% CO_2, while 500 μl RPMI-1640 with 10% FBS was added into the lower chamber as chemoattractant. After 24 h, the lower chamber was washed with PBS multiple times. The cells were then fixed by paraformaldehyde solution (4%) for 30 min and then stained by 0.1% Giemsa (G4640, Solarbio, China) for 20 min. Cell number was counted from five random fields under a stereo microscope (SZX10; Olympus, China) and photographed at 250× magnification.

Flow cytometry

The MCF7 cells (1×10^5) were treated with Annexin V and propidium iodide (PI) (5 μl for each) together for 15 min at room temperature in the dark. Next, the cells were collected and washed by cold PBS twice, and cell apoptosis was detected using Annexin V-FITC/PI cell apoptosis kit (KA3805, Abnova, Walnut, CA, U.S.A.). Cell apoptosis was detected by Guava easyCyte Benchtop Flow Cytometer (BR168323; Luminex, Austin, TX, U.S.A.). The data were analyzed using Kaluza C Analysis Software (Beckman Coulter, Indianapolis, IN, U.S.A.).

RNA isolation and qRT-PCR

Total RNAs were extracted from cells using TRIzol (A33250, Invitrogen, Carlsbad, CA, U.S.A.) and preserved at 4°C. Concentration of the total RNA was quantified with a biological spectrometer (Nano Drop 2000, Thermo Fisher Scientific, U.S.A.). One microgram of total RNA was used to synthesize cDNA using a First-strand cDNA Synthesis Kit (TB300001A, TonkBio, Parsippany, NJ, U.S.A.). qRT-PCR was performed using Easy-A One-Tube RT-PCR kit (600182, Agilent Technologies, Santa Clara, CA, U.S.A.) in real-time PCR Detection system (LineGene 9600 Plus; Biosan; Riga, Latvia) under the following conditions: 95°C for 15 min, followed by 40 cycles at 95°C for 30 s, 60°C for 30 s, and 68°C for 2 min. Primer sequences were listed in Table 1. GAPDH was used as the internal control. Relative gene expression was calculated by $2^{-\Delta\Delta C_T}$ calculation method [15].

Bioscience Reports (2020) **40** BSR20201854
https://doi.org/10.1042/BSR20201854

Table 1 Primers for qRT-PCR

Gene	Primers
PRR11	
Forward	5′-GAATCCACTAGTTACCGTCT-3′
Reverse	5′-GACTTTTCTAAGCAGTTTCC-3′
GAPDH	
Forward	5′-CCCCGGTTTCTATAAATTGAGC-3′
Reverse	5′-CTTTCCCCATGGTGTCTGAG-3′

Western blot

Western blot was performed to determine the protein expressions of PRR11 and genes related to epithelial-to-mesenchymal transition (EMT) and apoptosis [16]. The proteins were lysed and extracted by RIPA Lysis Buffer (76236-534, Agathos Scientific, Santa Clara, CA, U.S.A.) from the cells. Protein concentration was determined by bicinchoninic acid (BCA) protein kit (GK10009; GlpBio, Montclair, CA, U.S.A.). Sample lysates of protein (30 μg) were separated by 10% sodium dodecyl sulfate/polyacrylamide gel electrophoresis (SDS/PAGE; P0012A; Beyotime, Shanghai, China), and then transferred into Immun-Blot® polyvinylidene fluoride (PVDF) membrane (1620174; Bio-Rad, Hercules, CA, U.S.A.). The membrane was blocked with skimmed milk (5%) for 2 h and incubated with the following primary antibodies: anti-PRR11 antibody (rabbit, 1:5000, ab237526, Abcam, Shanghai, China), anti-E-cad (E-cadherin) antibody (rabbit, 1:10000, ab40772, Abcam, China), anti-N-cad (N-cadherin) antibody (rabbit, 1:1000, ab18203, Abcam, China), anti-Snail antibody (goat, 1:100, ab53519, Abcam, China), anti-Bcl-2 (B-cell lymphoma 2) antibody (rabbit, 1:1000, ab59348, Abcam, China), anti-Bax (Bcl-2-associated protein X) antibody (rabbit, 1:10000, ab32503, Abcam, China) and anti-GAPDH antibody (mouse, 1:10000, ab8245, Abcam, China) at 4°C overnight, and GAPDH was the internal control. Next, the membrane was incubated with the secondary horseradish peroxidase (HRP)-conjugated antibodies as follows: goat anti-rabbit IgG H&L (HRP) (1:5000, A00098, GenScript, Nanjing, China), donkey anti-goat IgG H&L (HRP) (1:5000, A00178, GenScript, China), and goat anti-mouse IgG H&L (HRP) (1:5000, A00160, GenScript, China) for 1 h at room temperature and washed using Tris-buffer saline Tween (TBST) for three times. Protein bands were collected and developed by enhanced chemiluminescence (ECL) Western Blotting kit (RPN2108; Global Life Sciences Solutions, Pittsburgh, PA, U.S.A.). Gray values of the strips were analyzed and calculated by ImageJ 5.0 (National Institutes of Health, Bethesda, MD, U.S.A.).

Statistical analysis

All the experiments have been independently performed in triplicate. The data were shown as mean ± standard deviation (SD). Analysis of statistics was performed using SPSS 20.0 software (IBM Corporation, Armonk, NY, U.S.A.). Statistical significances were assessed by one-way ANOVA and Student's *t* test. P-value<0.05 was considered as statistically significant.

Results

Effects of different ultrasonic intensities on MCF7 cells

To determine the optimal ultrasonic intensity on breast cancer MCF7 cells, the MCF7 cells were exposed to different ultrasonic intensities (0, 0.5, 0.75, 1, and 1.25 W/cm^2) for 45 s, and the viability was measured by MTT assay. As shown in Figure 1A, cell viability was decreased as the ultrasonic intensity increased, and 1.0 W/cm^2 showed the optimal suppressive effects on cells (Figure 1A, $P<0.05$). Therefore, ultrasonic intensity at 0.75 W/cm^2 was used for subsequent studies.

PRR11 expression was up-regulated in breast cancer tissues

To investigate the role of PRR11 in breast cancer, the expression of PRR11 was obtained from GEPIA, and the data showed that PRR11 expression was up-regulated in breast cancer tissues (Figure 1B, number of tumor (T) = 1085, number of normal (N) = 291, $P<0.05$), suggesting that PRR11 may promote breast cancer development and progression.

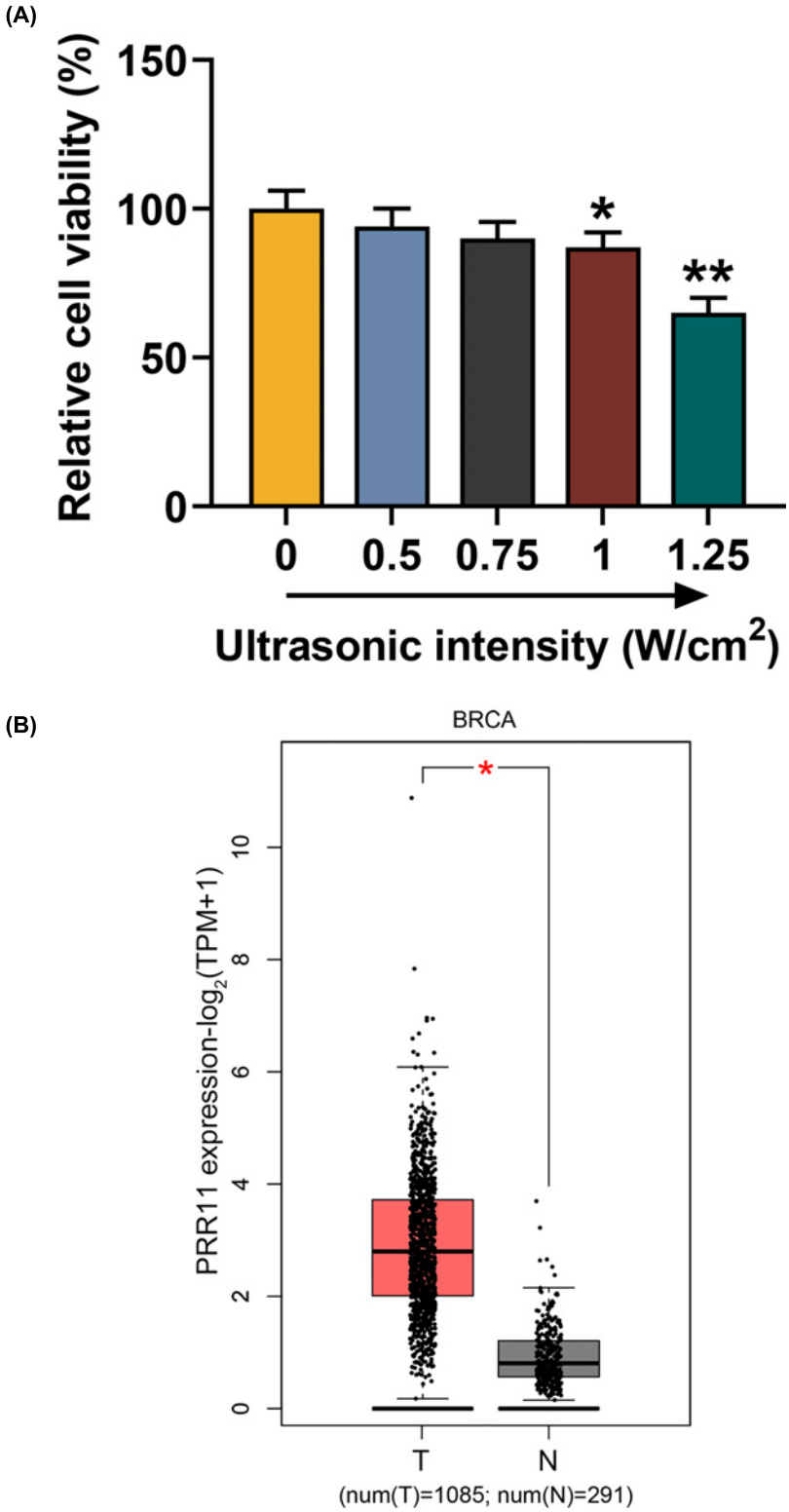

Figure 1. Human breast cancer MCF7 cells viability was decreased as ultrasonic intensity increased, and PRR11 expression was up-regulated in BRCA

(**A**) MCF7 cells' viability after exposure to different ultrasonic intensities (0, 0.5, 0.75, 1, and 1.25 W/cm^2) was measured with MTT assay. (**B**) Data on PRR11 expressions in breast cancer tissues (T) and normal tissues (N) were retrieved from GEPIA (T = 1085, N = 291). All experiments have been performed in triplicate and experimental data were expressed as mean ± SD. *P<0.05, **P<0.01, vs. 0 W/cm^2.

Bioscience Reports (2020) **40** BSR20201854
https://doi.org/10.1042/BSR20201854

Effects of transfection mediated by US and Lipofectamine 3000 on PRR11 expression in cells

To examine the effects of using Lipofectamine 3000 (L) or US for the transfection of siPRR11 and overexpressed PRR11 into the cells, we first measured the transfection efficiency by Western blot and qRT-PCR. As shown in Figure 2A–D, both expressions of PRR11 protein and mRNA were down-regulated after transfection of siPRR11, whereas PRR11 overexpression increased protein and mRNA expressions of PRR11 (Figure 2A–D, $P<0.05$). In addition, after transfection of PRR11 overexpression plasmid using US, protein, and mRNA expressions of PRR11 were low, whereas a PRR11 protein and mRNA expressions were high (Figure 2A–D, $P<0.01$), suggesting that siPRR11 or overexpressed PRR11 plasmid transfected by US produced better effects on PRR11 expression in the cells, as compared with transfection using Lipofectamine 3000 reagent.

Effects of transfection mediated by US and Lipofectamine 3000 on the viability and proliferation of the cells

After the transfection of siPRR11 and overexpressed PRR11, the viability of MCF7 cells was measured by MTT assay, and we found that MCF7 cell viability was decreased after the transfection of siPRR11, while PRR11 overexpression caused increased MCF7 cell viability (Figure 2E,F, $P<0.05$). Also, cell viability after transfection of siPRR11 using US was lower, but transfection of PRR11 overexpression plasmid using US resulted in a higher cell viability (Figure 2E,F, $P<0.05$).

In clone formation assay, we found that the rate of colony formed was decreased after siPRR11 transfection, which was increased by PRR11 overexpression (Figure 3A,B, $P<0.01$). Meanwhile, colony formation rate was lower after the transfection of siPRR11 using US, while transfection of PRR11 overexpression plasmid using US resulted in a higher colony formation rate (Figure 3A,B, $P<0.01$). These results suggested that transfection of siPRR11 or overexpressed PRR11 plasmid using US had better effects on the viability and proliferation of the cells, as compared with transfection using Lipofectamine 3000 reagent.

Effects of transfection mediated by US and Lipofectamine 3000 on the migration and invasion of the cells

The migration of MCF7 cells was measured after the transfection of siPRR11 and overexpressed PRR11 using scratch assay. We found that MCF7 cell migration rate was decreased after the transfection of siPRR11, while PRR11 overexpression increased MCF7 cell migration (Figure 4A–D, $P<0.01$). Also, the cell migration after transfection of siPRR11 using US was lower, but transfection of PRR11 overexpression plasmid using US caused a higher cell migration (Figure 4A–D, $P<0.01$).

Transwell assay showed that after siPRR11 transfection, cell invasion was decreased, while PRR11 overexpression plasmid transfection increased cell invasion (Figure 4E-H, $P<0.01$). Meanwhile, cell invasion was lower after the transfection of siPRR11 using US, but transfection of PRR11 overexpression plasmid US caused a higher cell invasion (Figure 4E-H, $P<0.01$). In conclusion, transfection with US showed a better effect on cell migration and invasion, as compared with transfection using Lipofectamine 3000 reagent.

Effects of transfection mediated by US and Lipofectamine 3000 on the cell apoptosis

Flow cytometry showed that after siPRR11 transfection, cell apoptosis rate was increased, while PRR11 overexpression reduced cell apoptosis rate (Figure 5A,B, $P<0.05$). Meanwhile, cell apoptosis became higher after the transfection of siPRR11 using US, but transfection of PRR11 overexpression plasmid using US reduced the cell apoptosis (Figure 5A,B, $P<0.001$). These results suggested that transfection with US showed better effect on cells apoptosis, as compared with transfection with Lipofectamine 3000 reagent.

Effects of transfection mediated by US and Lipofectamine 3000 on the expressions of EMT- and apoptosis-related proteins

Western blot was performed to measure the expressions of EMT- and apoptosis-related proteins. The results showed that after siPRR11 transfection, the protein expressions of E-cad and Bax were increased, but the expressions of N-cad, Snail, and Bcl-2 were decreased, however, PRR11 overexpression resulted in different results (Figure 6A,B, $P<0.05$). Meanwhile, higher protein expressions of E-cad and Bax and lower expressions of N-cad, Snail, and Bcl-2 expressions were observed after the transfection of siPRR11 using US. However, transfection of PRR11 overexpression plasmid

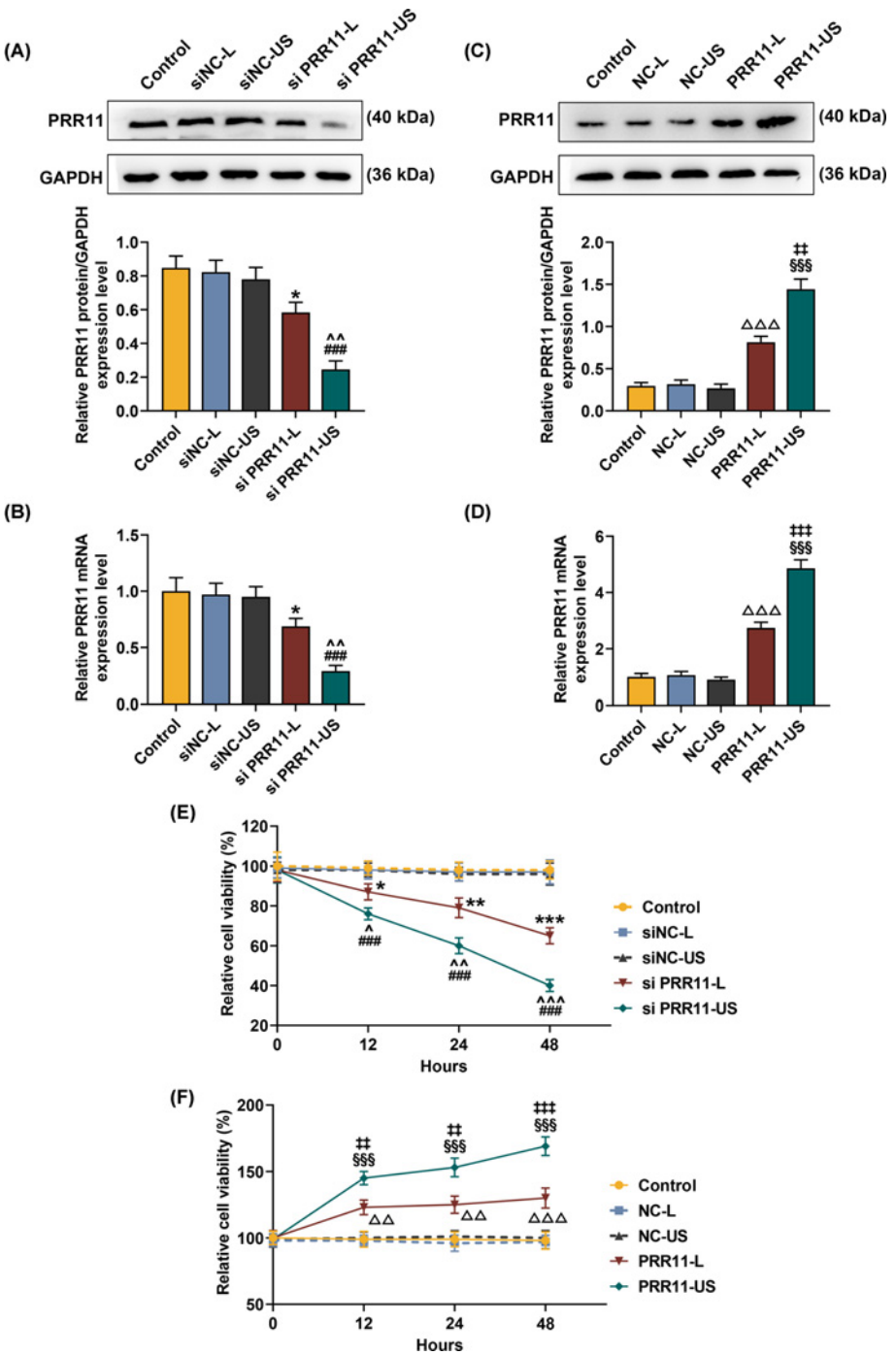

Figure 2. Effects of siPRR11 and overexpressed PRR11 transfection mediated by Lipofectamine 3000 and US on PRR11 expression and viability of MCF7 cells

(**A**,**B**) After 48-h transfection, relative protein/GAPDH and mRNA expressions of PRR11 after siPRR11 transfection were measured by Western blot and qRT-PCR. GAPDH was the internal control. (**C**,**D**) After 48 h transfection, relative protein/GAPDH and mRNA expressions of PRR11 after PRR11 overexpression plasmid transfection were measured by Western blot and qRT-PCR. GAPDH was the internal control. (**E**) Relative MCF7 cell viability after siPRR11 transfection was detected with MTT assay after transfection for 12, 24, and 48 h. (**F**) Relative MCF7 cell viability after PRR11 overexpression plasmid transfection was detected with MTT assay after transfection for 12, 24, and 48 h. All experiments have been performed in triplicate and experimental data were expressed as mean ± standard deviation (SD). $^{*}P<0.05$, $^{**}P<0.01$, $^{***}P<0.001$, vs. siNC-L; $^{\#\#}P<0.01$, $^{\#\#\#}P<0.001$, vs. siNC-US; $^{\wedge}P<0.05$, $^{\wedge\wedge}P<0.01$, $^{\wedge\wedge\wedge}P<0.001$, vs. siPRR11-L; $^{\triangle\triangle}P<0.01$, $^{\triangle\triangle\triangle}P<0.001$, vs. NC-L; $^{\S\S\S}P<0.001$, vs. NC-US; $^{\ddagger}P<0.05$, $^{\ddagger\ddagger}P<0.01$, $^{\ddagger\ddagger\ddagger}P<0.001$, vs. PRR11-L. Abbreviation: L, Lipofectamine 3000.

Bioscience Reports (2020) **40** BSR20201854
https://doi.org/10.1042/BSR20201854

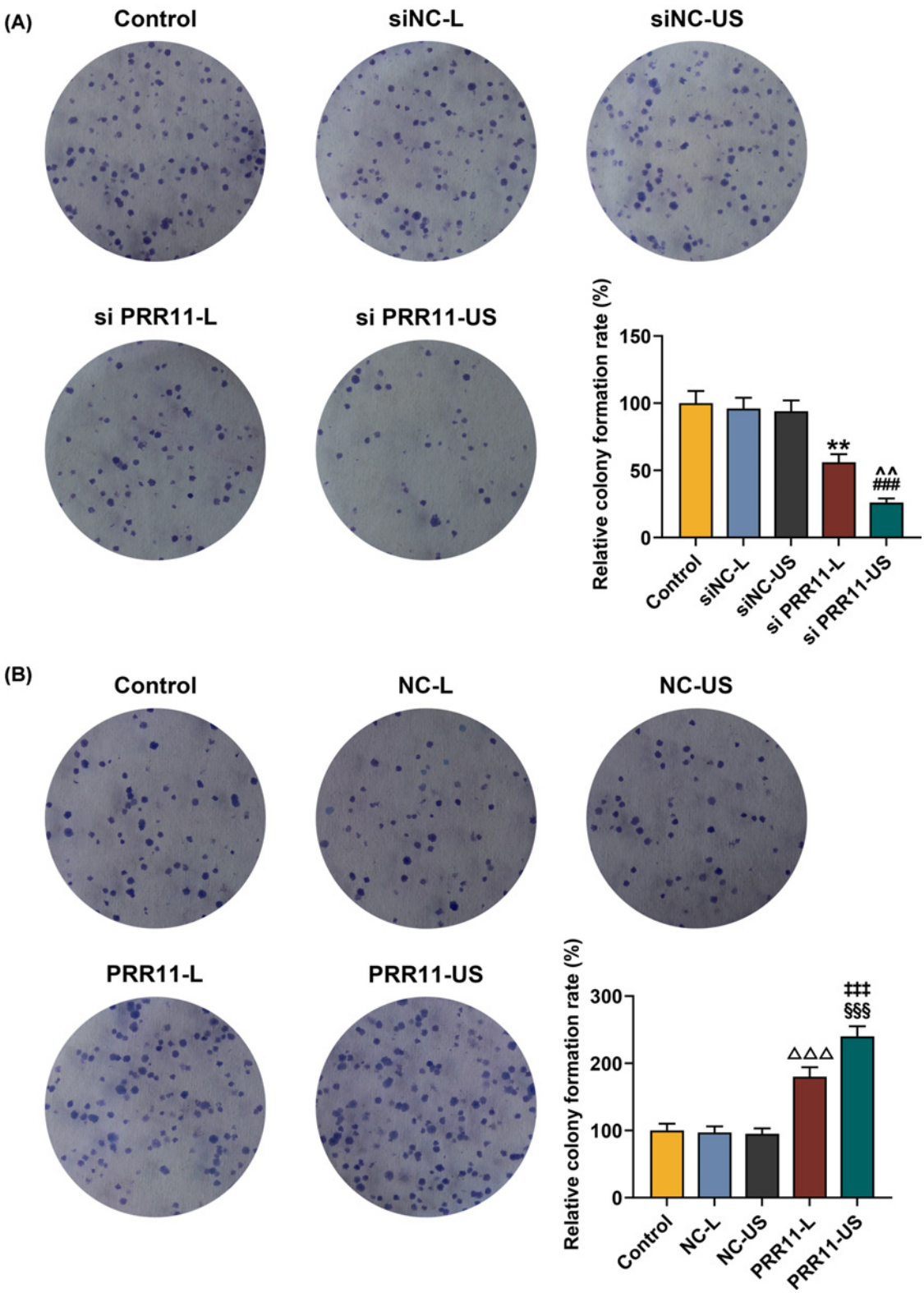

Figure 3. Effects of siPRR11 and overexpressed PRR11 mediated by Lipofectamine 3000 and US on MCF7 cell proliferation

(**A**) Relative colony formation rate of MCF7 cell after siPRR11 transfection were detected with clone formation assay. (**B**) Relative colony formation rate of MCF7 cell after PRR11 overexpression plasmid transfection were detected with clone formation assay. All experiments have been performed in triplicate and experimental data were expressed as mean ± SD. $^{**}P<0.01$, vs. siNC-L; $^{\#\#\#}P<0.001$, vs. siNC-US; $^{\wedge\wedge}P<0.01$, vs. siPRR11-L; $^{\triangle\triangle\triangle}P<0.001$, vs. NC-L; $^{\S\S\S}P<0.001$, vs. NC-US; $^{\ddagger\ddagger\ddagger}P<0.001$, vs. PRR11-L.

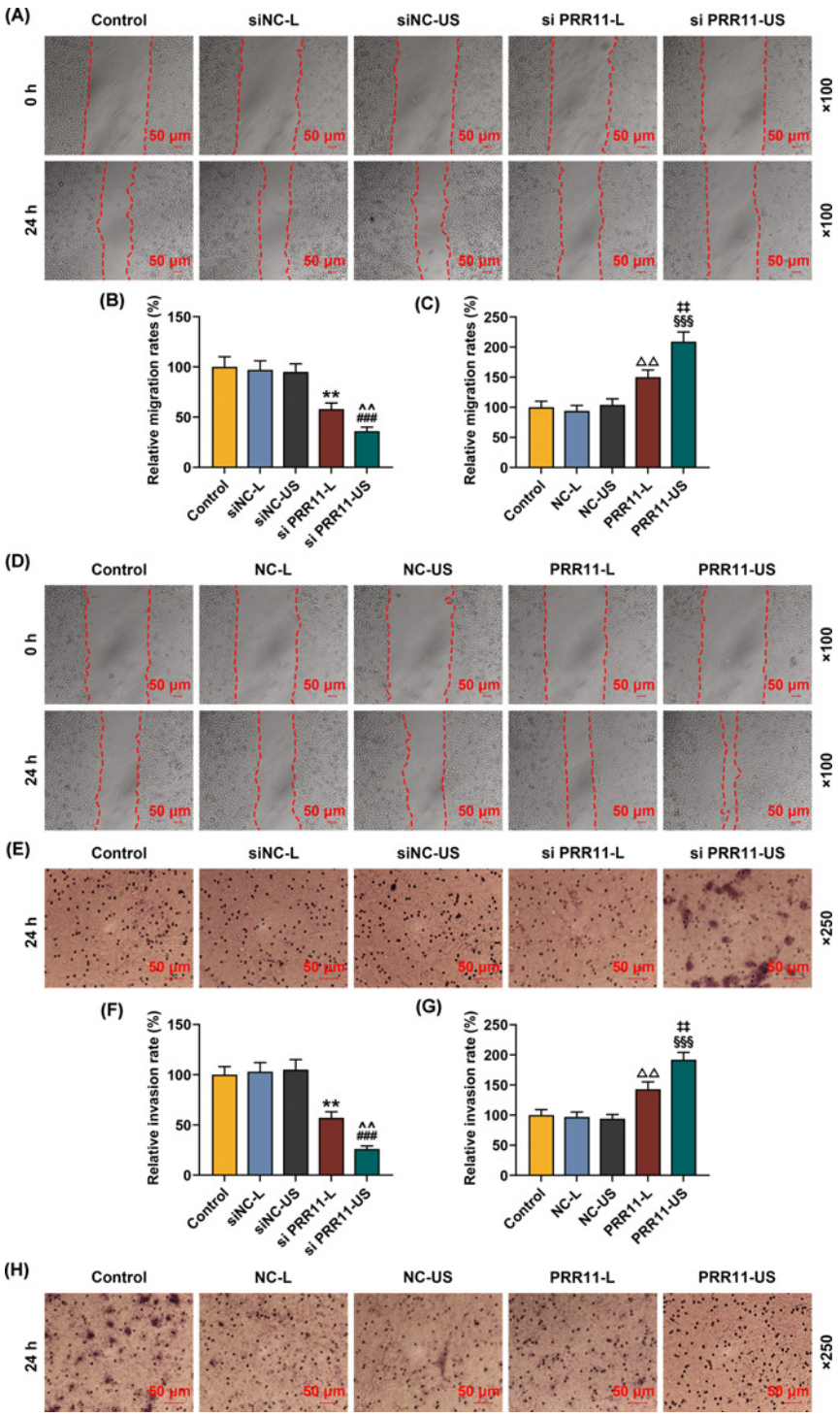

Figure 4. Effects of siPRR11 and overexpressed PRR11 transfection mediated by Lipofectamine 3000 and US on MCF7 cell migration and invasion

(**A**,**B**) Relative migration rate of MCF7 cell after siPRR11 transfection were measured by scratch assay, at 0 and 24 h, under 100× magnification. (**C**,**D**) Relative migration rate of MCF7 cell after PRR11 overexpression plasmid transfection were quantified with scratch assay at 0 and 24 h, under 100× magnification. (**E**,**F**) Relative invasion rate of MCF7 cell after siPRR11 transfection were measured with Transwell assay at 24 h, under 250× magnification. (**G**,**H**) Relative invasion rate of MCF7 cell after PRR11 overexpression plasmid transfection were measured with Transwell assay at 24 h, under 250× magnification. All experiments have been performed in triplicate and experimental data were expressed as mean ± SD. $^{**}P<0.01$, vs. siNC-L; $^{\#\#\#}P<0.001$, vs. siNC-US; $^{\wedge\wedge}P<0.01$, vs. siPRR11-L; $^{\triangle\triangle}P<0.01$, $^{\triangle\triangle\triangle}P<0.001$, vs. NC-L; $^{\S\S\S}P<0.001$, vs. NC-US; $^{\ddagger\ddagger}P<0.01$, $^{\ddagger\ddagger\ddagger}P<0.001$, vs. PRR11-L.

Bioscience Reports (2020) **40** BSR20201854
https://doi.org/10.1042/BSR20201854

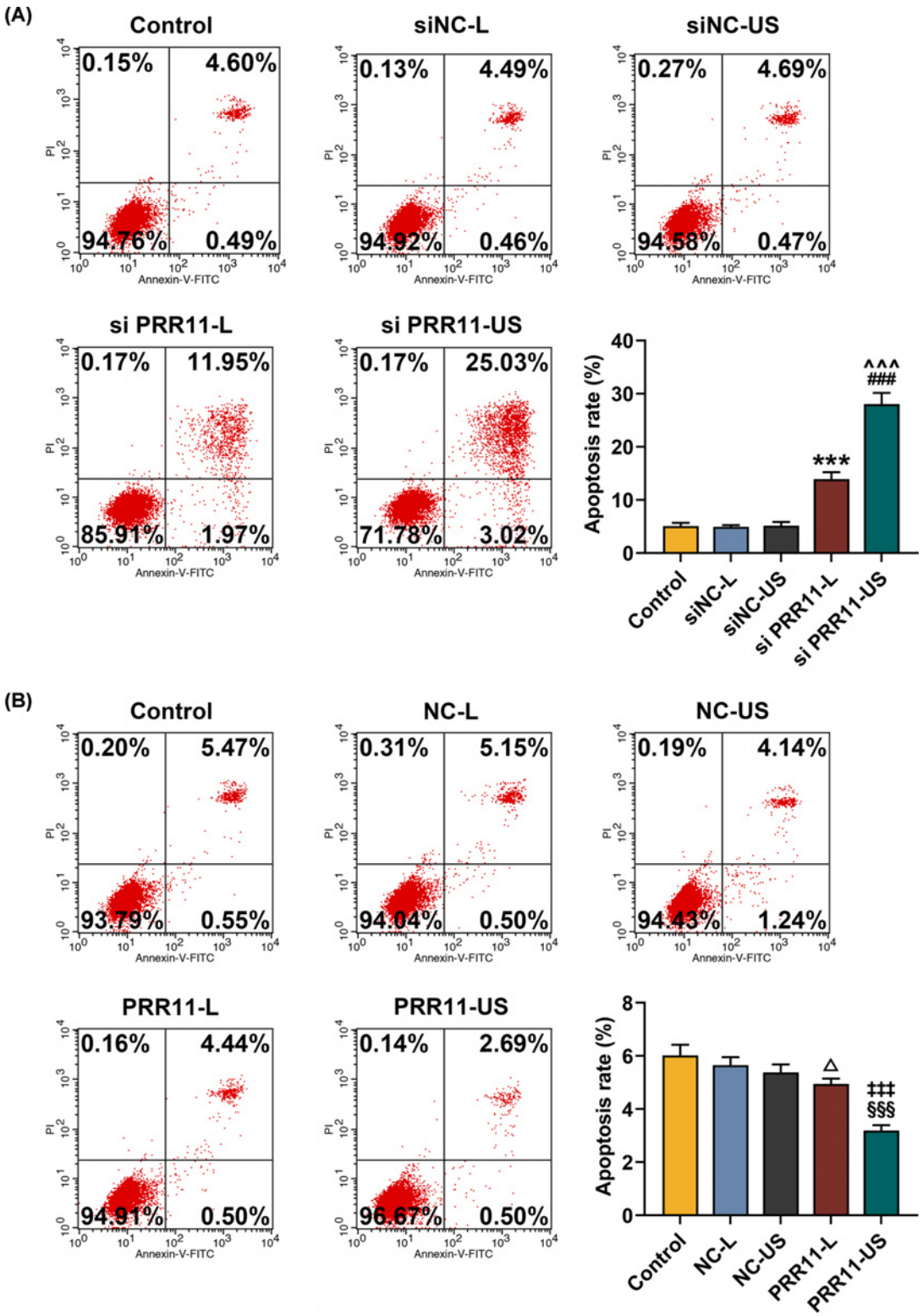

Figure 5. Effects of siPRR11 and overexpressed PRR11 transfection mediated by Lipofectamine 3000 and US on MCF7 cell apoptosis

(**A**) Relative apoptosis rate of MCF7 cell after siPRR11 transfection were measured by flow cytometry. (**B**) Relative apoptosis rate of MCF7 cell after PRR11 overexpression plasmid transfection were measured by flow cytometry. All experiments have been performed in triplicate and experimental data were expressed as mean ± SD. $^{***}P<0.001$, vs. siNC-L; $^{\#\#\#}P<0.001$, vs. siNC-US; $^{\wedge\wedge\wedge}P<0.001$, vs. siPRR11-L; $^{\triangle}P<0.05$, vs. NC-L; $^{\S\S\S}P<0.001$, vs. NC-US; $^{\ddagger\ddagger\ddagger}P<0.001$, vs. PRR11-L.

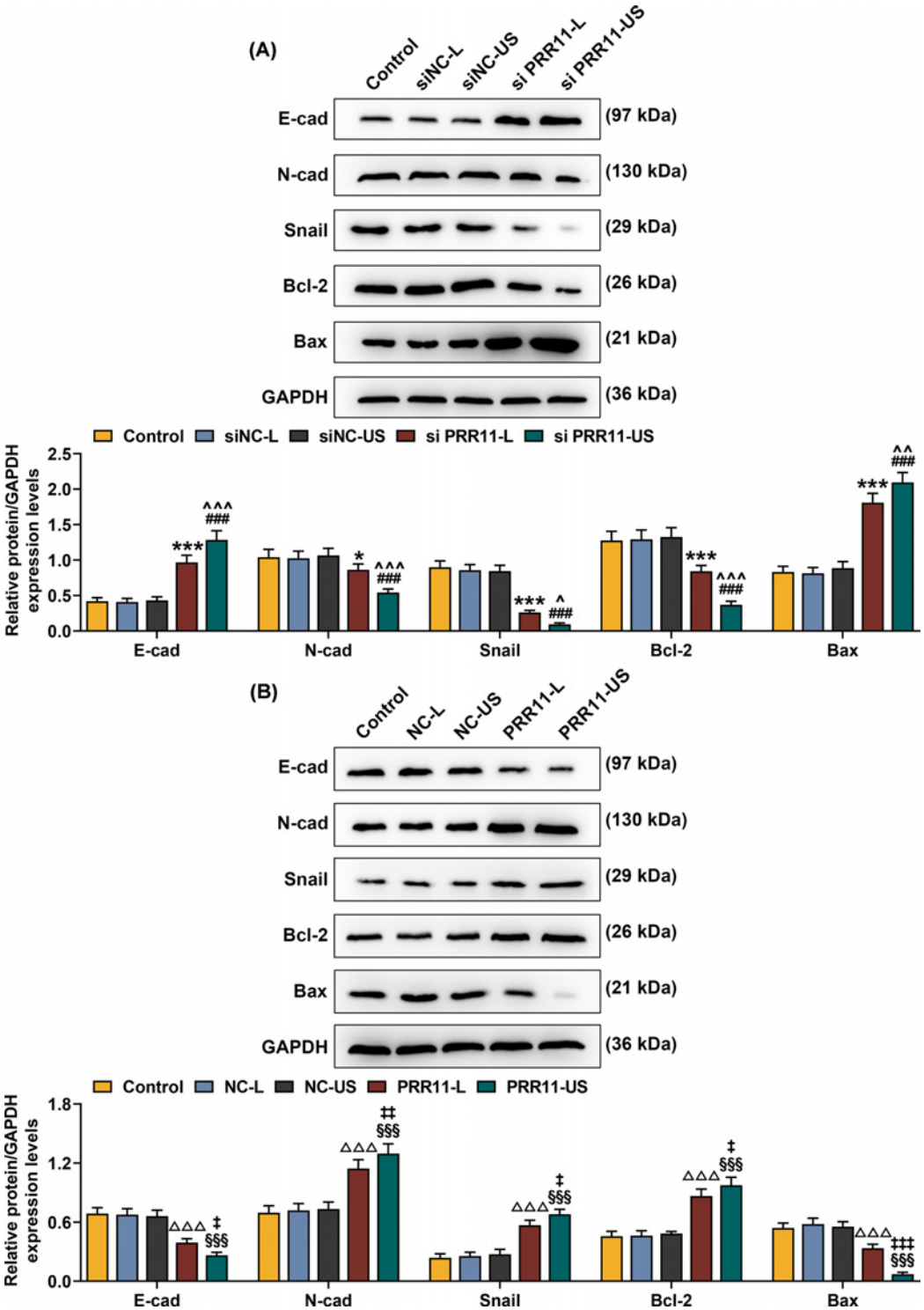

Figure 6. Effects of siPRR11 and overexpressed PRR11 transfection mediated by Lipofectamine 3000 and US on EMT- and apoptosis-related genes protein expressions

(**A**) Relative protein/GAPDH expressions of E-cad, N-cad, Snail, Bcl-2, and Bax after siPRR11 transfection were measured by Western blot. GAPDH was an internal control. (**B**) Relative protein/GAPDH expressions of E-cad, N-cad, Snail, Bcl-2, and Bax after PRR11 overexpression plasmid transfection were measured by Western blot. GAPDH was the internal control. All experiments have been performed in triplicate and experimental data were expressed as mean ± SD. $^{*}P<0.05$, $^{***}P<0.001$, vs. siNC-L; $^{\#\#\#}P<0.001$, vs. siNC-US; $^{\wedge}P<0.05$, $^{\wedge\wedge}P<0.01$, $^{\wedge\wedge\wedge}P<0.001$, vs. siPRR11-L; $^{\triangle\triangle\triangle}P<0.001$, vs. NC-L; $^{\S\S\S}P<0.001$, vs. NC-US; $^{\ddagger}P<0.05$, $^{\ddagger\ddagger}P<0.01$, $^{\ddagger\ddagger\ddagger}P<0.001$, vs. PRR11-L.

Bioscience Reports (2020) **40** BSR20201854
https://doi.org/10.1042/BSR20201854

using US resulted in opposite results (Figure 6A,B, $P<0.05$). These results revealed that transfection mediated by US produced a better effect on cell migration and invasion, as compared with transfection with Lipofectamine 3000 reagent.

Discussion

Gene therapy has been increasingly applied to treat human malignancies [17]. PRR11, a cell cycle-dependent gene, acts as an oncogene in the development and progression of a variety of cancers including in breast cancer [6]. We also found that PRR11 expression was up-regulated in breast cancer tissues, and silencing PRR11 suppressed the proliferation and metastasis of breast cancer cells and promoted apoptosis. The current study was the first to demonstrate that PRR11 knockdown and overexpression mediated by with US had better effects on breast cancer cells as compared with transfection with Liposome.

Antisense DNA or siRNA has promising preclinical results on suppressing the expression of a target gene, and different from unlike traditional medication, gene silencing through RNA interference (RNAi) using viral vectors can suppress targeted genes with a high selectivity and great potency [14]. However, the application of viral vectors has also stimulated great concern over its safety and efficiency due, as it could cause toxicity, immunogenicity, and tumorigenicity [18]. Compared with viral vectors, microbubble ultrasound contrast agents have higher efficiency, fewer side-effects and better targeting effects, suggesting that it could be used as a novel targeting gene transfection system [19]. The ultrasound intensity could be easily controlled, making it easy to break microbubbles and release target genes at the designated time and place [20]. Also, microbubbles could travel through lung and respiratory system and have fewer side effects [11]. Moreover, as compared with liposome, the transfection efficiency has been proven to have better effects [21]. Therefore, gene transfection with microbubble ultrasound contrast agent could be used in the future.

Previous study suggested that PRR11 could promote the metastasis of breast cancer cells though the regulation of EMT [22]. In the present study, PRR11 was transfected using US, and its effects were better than transfection using liposome. The results also showed that silencing PRR11 suppressed the proliferation and metastasis of breast cancer cells and promoted apoptosis, moreover, the transfection with US further enhanced the effects.

EMT is in many diseases including in cancers. EMT is characterized by loss or dysfunction of E-cad expression and increased expressions of Snail and N-cad [23,24]. E-cad is an adhesion molecule regulated by calcium and is expressed in most epithelial tissues, and loss of E-cad was related to the dedifferentiation and invasiveness of human malignancies [25]. Snail acts as a pivotal repressor of E-cad during EMT and plays a vital role in cancer progression [26]. N-cad was lowly expressed in epithelial cells in normal state, and aberrant N-cad expression is related to the progression of malignancies [27]. Previous study indicated that silencing PRR11 could up-regulate E-cad expression and down-regulate N-cad and Snail expressions in hepatocellular carcinoma [3]. We found that after silencing PRR11 by Liposome transfection, E-cad expression was up-regulated and Snail and N-cad expressions were down-regulated in breast cancer cells, and siPRR11 transfection with microbubble and ultrasound further enhanced the effects, suggesting that siPRR11 transfection with microbubble and ultrasound suppressed breast cancer cell metastasis *in vitro*.

Regulation of the proliferation of cancer cells is often achieved with the modulation on the critical factors, such as Bcl-2 and Bax, which are two cell apoptosis-related genes [28]. Bcl-2 could suppress cell apoptosis either through preventing the release of cytochrome *c* from mitochondria or through binding with the apoptosis-activating factor (APAF-1) [29]. Bax could form the heterodimer with Bcl-2 to prevent the suppressive function of Bcl-2 on apoptosis [30]. The current study was the first to discover that silencing PRR11 down-regulated Bcl-2 expression and up-regulated Bax expression, and siPRR11 transfection with microbubble and ultrasound further enhanced such effects, suggesting that siPRR11 transfection with microbubble and ultrasound could promote the apoptosis of breast cancer cells *in vitro*.

There existed some limitations in our present research. We only examined one breast cancer cell line MCF7 *in vitro*, thus the current results should be verified in more breast cancer cell lines Also, the efficacy of transfection with microbubble and ultrasound needed to be further verified *in vivo*.

In conclusion, siPRR11 was transfected using microbubble and ultrasound into breast cancer cells *in vitro*, and the result indicated that silencing PRR11 could suppress the proliferation and metastasis but promoted apoptosis of breast cancer cells. Meanwhile, we also found that siPRR11 transfection with microbubble and ultrasound further enhanced the effects of silencing PRR11 on breast cancer cells, showing that siPRR11 transfection with microbubble and ultrasound could be used as a possible therapeutic method for treating breast cancer treatment.

Competing Interests

The authors declare that there are no competing interests associated with the manuscript.

Funding

This work was supported by the National Natural Science Foundation of China [grant number 81771841]; and the Clinical Project of Shenzhen People's Hospital [grant number SYLY201903].

Author Contribution

Substantial contributions to conception and design: H.L. and J.L. Data acquisition, data analysis and interpretation: Q.L., X.X., Y.S., X.Y., Z.W., Y.L., and J.X. Drafting the article or critically revising it for important intellectual content: H.L. and J.L. Final approval of the version to be published: all authors. Agreement to be accountable for all aspects of the work in ensuring that questions related to the accuracy or integrity of the work are appropriately investigated and resolved: all authors.

Abbreviations

Bax, Bcl-2-associated protein X; Bcl-2, B-cell lymphoma 2; EMT, epithelial-to-mesenchymal transition; E-cad, E-cadherin; FBS, fetal bovine serum; GAPDH, glyceraldehyde-3-phosphate dehydrogenase; GEPIA, Gene Expression Profiling Interactive Analysis; HRP, horseradish peroxidase; MTT, 3-(4,5)-dimethylthiahiazo (-z-y1)-3,-di-phenytetrazoliumromide; NC, negative control; NSCLC, non-small cell lung cancer; N-cad, N-cadherin; OD, optical density; PI, propidium iodide; PRR11, proline-rich protein 11; qRT-PCR, quantitative real-time polymerase chain reaction; RPMI, Roswell Park Memorial Institute; siNC, small interfering RNA for NC; siPRR11, small interfering RNA for PRR11; US, ultrasonic irradiation and SonoVue microbubbles.

References

1 Ma, D., Chen, C., Wu, J., Wang, H. and Wu, D. (2019) Up-regulated lncRNA AFAP1-AS1 indicates a poor prognosis and promotes carcinogenesis of breast cancer. *Breast Cancer* **26**, 74–83, https://doi.org/10.1007/s12282-018-0891-3
2 Peart, O. (2017) Metastatic breast cancer. *Radiol. Technol.* **88**, 519M–539M
3 Qiao, W., Wang, H., Zhang, X. and Luo, K. (2019) Proline-rich protein 11 silencing inhibits hepatocellular carcinoma growth and epithelial-mesenchymal transition through beta-catenin signaling. *Gene* **681**, 7–14, https://doi.org/10.1016/j.gene.2018.09.036
4 Huang, Y., Ni, R., Wang, J. and Liu, Y. (2019) Knockdown of lncRNA DLX6-AS1 inhibits cell proliferation, migration and invasion while promotes apoptosis by downregulating PRR11 expression and upregulating miR-144 in non-small cell lung cancer. *Biomed. Pharmacother.* **109**, 1851–1859, https://doi.org/10.1016/j.biopha.2018.09.151
5 Wang, C., Yu, L., Hu, F., Wang, J., Chen, X., Tai, S. et al. (2017) Upregulation of proline rich 11 is an independent unfavorable prognostic factor for survival of tongue squamous cell carcinoma patients. *Oncol. Lett.* **14**, 4527–4534, https://doi.org/10.3892/ol.2017.6780
6 Wang, Y., Zhang, C., Mai, L., Niu, Y., Wang, Y. and Bu, Y. (2019) PRR11 and SKA2 gene pair is overexpressed and regulated by p53 in breast cancer. *BMB Rep.* **52**, 157–162, https://doi.org/10.5483/BMBRep.2019.52.2.207
7 Foldvari, M., Chen, D.W., Nafissi, N., Calderon, D., Narsineni, L. and Rafiee, A. (2016) Non-viral gene therapy: gains and challenges of non-invasive administration methods. *J. Control. Release* **240**, 165–190, https://doi.org/10.1016/j.jconrel.2015.12.012
8 Guo, X., Guo, S., Pan, L., Ruan, L., Gu, Y. and Lai, J. (2017) Anti-microRNA-21/221 and microRNA-199a transfected by ultrasound microbubbles induces the apoptosis of human hepatoma HepG2 cells. *Oncol. Lett.* **13**, 3669–3675, https://doi.org/10.3892/ol.2017.5910
9 Wu, B., Qiao, Q., Han, X., Jing, H., Zhang, H., Liang, H. et al. (2016) Targeted nanobubbles in low-frequency ultrasound-mediated gene transfection and growth inhibition of hepatocellular carcinoma cells. *Tumour Biol.* **37**, 12113–12121, https://doi.org/10.1007/s13277-016-5082-2
10 Xie, A., Wu, M.D., Cigarroa, G., Belcik, J.T., Ammi, A., Moccetti, F. et al. (2016) Influence of DNA-microbubble coupling on contrast ultrasound-mediated gene transfection in muscle and liver. *J. Am. Soc. Echocardiogr.* **29**, 812–818, https://doi.org/10.1016/j.echo.2016.04.011
11 Yamaguchi, H., Ishida, Y., Hosomichi, J., Suzuki, J.I., Hatano, K., Usumi-Fujita, R. et al. (2017) Ultrasound microbubble-mediated transfection of NF-kappaB decoy oligodeoxynucleotide into gingival tissues inhibits periodontitis in rats in vivo. *PLoS ONE* **12**, e0186264, https://doi.org/10.1371/journal.pone.0186264
12 He, X., Wu, D.F., Ji, J., Ling, W.P., Chen, X.L. and Chen, Y.X. (2016) Ultrasound microbubble-carried PNA targeting to c-myc mRNA inhibits the proliferation of rabbit iliac arterious smooth muscle cells and intimal hyperplasia. *Drug Deliv.* **23**, 2482–2487, https://doi.org/10.3109/10717544.2015.1014947
13 Hou, L., Chen, M., Yang, H., Xing, T., Li, J., Li, G. et al. (2016) MiR-940 inhibited cell growth and migration in triple-negative breast cancer. *Med. Sci. Monit.* **22**, 3666–3672, https://doi.org/10.12659/MSM.897731
14 Ran, L.W., Wang, H., Lan, D., Jia, H.X. and Yu, S.S. (2018) Effect of RNA interference targeting STAT3 gene combined with ultrasonic irradiation and SonoVue microbubbles on proliferation and apoptosis in keratinocytes of psoriatic lesions. *Chin. Med. J. (Engl.)* **131**, 2097–2104, https://doi.org/10.4103/0366-6999.239297
15 Livak, K.J. and Schmittgen, T.D. (2001) Analysis of relative gene expression data using real-time quantitative PCR and the 2(-Delta Delta C(T)) Method. *Methods* **25**, 402–408, https://doi.org/10.1006/meth.2001.1262
16 Zhang, L., Zhang, Y., Lei, Y., Li, Y., Wei, Z., Wang, Y. et al. (2020) Proline rich 11 drives F-actin assembly by recruiting the actin-related protein 2/3 complex in human non-small cell lung carcinoma. *J. Biol. Chem.* **295**, 5335–5349, https://doi.org/10.1074/jbc.RA119.012260

17 Friedmann, T. (2019) Genetic therapies, human genetic enhancement, and . . . eugenics? *Gene Ther.* **26**, 351–353, https://doi.org/10.1038/s41434-019-0088-1
18 Nie, F., Wang, X.F., Zhao, S.Y., Bu, L. and Liu, X.H. (2015) Gene silencing of Rac1 with RNA interference mediated by ultrasound and microbubbles in human LoVo cells: evaluation of cell invasion inhibition and metastatic. *J. Drug Target* **23**, 380–386, https://doi.org/10.3109/1061186X.2014.1002500
19 Shentu, W.H., Yan, C.X., Liu, C.M., Qi, R.X., Wang, Y., Huang, Z.X. et al. (2018) Use of cationic microbubbles targeted to P-selectin to improve ultrasound-mediated gene transfection of hVEGF165 to the ischemic myocardium. *J. Zhejiang Univ. Sci. B* **19**, 699–707, https://doi.org/10.1631/jzus.B1700298
20 Gong, L., Jiang, C., Liu, L., Wan, S., Tan, W., Ma, S. et al. (2018) Transfection of neurotrophin-3 into neural stem cells using ultrasound with microbubbles to treat denervated muscle atrophy. *Exp. Ther. Med.* **15**, 620–626
21 Huang, C., Zhang, H. and Bai, R. (2017) Advances in ultrasound-targeted microbubble-mediated gene therapy for liver fibrosis. *Acta Pharm. Sin. B* **7**, 447–452, https://doi.org/10.1016/j.apsb.2017.02.004
22 Yang, H., Zhou, L., Chen, J., Su, J., Shen, W., Liu, B. et al. (2019) A four-gene signature for prognosis in breast cancer patients with hypermethylated IL15RA. *Oncol. Lett.* **17**, 4245–4254
23 Chen, T., You, Y., Jiang, H. and Wang, Z.Z. (2017) Epithelial-mesenchymal transition (EMT): A biological process in the development, stem cell differentiation, and tumorigenesis. *J. Cell. Physiol.* **232**, 3261–3272, https://doi.org/10.1002/jcp.25797
24 Araki, K., Shimura, T., Suzuki, H., Tsutsumi, S., Wada, W., Yajima, T. et al. (2011) E/N-cadherin switch mediates cancer progression via TGF-beta-induced epithelial-to-mesenchymal transition in extrahepatic cholangiocarcinoma. *Br. J. Cancer* **105**, 1885–1893, https://doi.org/10.1038/bjc.2011.452
25 Singhai, R., Patil, V.W., Jaiswal, S.R., Patil, S.D., Tayade, M.B. and Patil, A.V. (2011) E-Cadherin as a diagnostic biomarker in breast cancer. *N Am. J. Med. Sci.* **3**, 227–233, https://doi.org/10.4297/najms.2011.3227
26 Wang, Y., Shi, J., Chai, K., Ying, X. and Zhou, B.P. (2013) The role of snail in EMT and tumorigenesis. *Curr. Cancer Drug Targets* **13**, 963–972, https://doi.org/10.2174/15680096113136660102
27 Mrozik, K.M., Blaschuk, O.W., Cheong, C.M., Zannettino, A.C.W. and Vandyke, K. (2018) N-cadherin in cancer metastasis, its emerging role in haematological malignancies and potential as a therapeutic target in cancer. *BMC Cancer* **18**, 939, https://doi.org/10.1186/s12885-018-4845-0
28 Xiao, X., Zhang, Y., Lin, Q. and Zhong, K. (2019) The better effects of microbubble ultrasound transfection of miR-940 on cell proliferation inhibition and apoptosis promotion in human cervical cancer cells. *Onco. Targets Ther.* **12**, 6813–6824, https://doi.org/10.2147/OTT.S209692
29 Wang, Y., Sun, Z.Y., Zhang, K.M., Xu, G.Q. and Li, G. (2011) Bcl-2 in suppressing neuronal apoptosis after spinal cord injury. *World J. Emerg. Med.* **2**, 38–44
30 Tirapelli, D., Lustosa, I.L., Menezes, S.B., Franco, I.M., Rodrigues, A.R., Peria, F.M. et al. (2017) High expression of XIAP and Bcl-2 may inhibit programmed cell death in glioblastomas. *Arq. Neuropsiquiatr.* **75**, 875–880, https://doi.org/10.1590/0004-282x20170156